Available online at www.sciencedirect.com
SCIENCE DIRECT
Biosensors and Bioelectronics 20 (2005) 1417–1421
BIOSENSORS BIOELECTRONICS
www.elsevier.com/locate/bios

Short communication

Integration of microfluidics with a four-channel integrated optical Young interferometer immunosensor

A. Ymeti [a,*], J.S. Kanger [b], J. Greve [a,b], G.A.J. Besselink [a], P.V. Lambeck [c], R. Wijn [d], R.G. Heideman [d]

[a] *Biophysical Techniques, Faculty of Science and Technology, MESA+ Institute for Nanotechnology, University of Twente, P.O. Box 217, 7500 AE Enschede, The Netherlands*
[b] *Biophysical Techniques, Faculty of Science and Technology, BMTI Institute, University of Twente, P.O. Box 217, 7500 AE Enschede, The Netherlands*
[c] *Integrated Optical Microsystems, Faculty of Electrical Engineering, Mathematics and Computer Science, MESA+ Institute for Nanotechnology, University of Twente, P.O. Box 217, 7500 AE Enschede, The Netherlands*
[d] *LioniX b.v., P.O. Box 456, 7500 AH Enschede, The Netherlands*

Received 20 February 2004; received in revised form 8 April 2004; accepted 15 April 2004
Available online 24 May 2004

Abstract

This report describes an optical sensing hybrid system obtained by bonding a microfluidic system to an integrated optical (IO) four-channel Young interferometer (YI) chip. The microfluidic system implemented into a glass plate consists of four microchannels with cross-sectional dimensions of 200 μm × 15 μm. The microfluidic system is structured in such a way that after bonding to the IO chip, each microchannel addresses one sensing window in the four-channel YI sensor. Experimental tests show that the implementation of the microfluidics reduces the response time of the sensor from 100 s, as achieved with a bulky cuvette, to 4 s. Monitoring the anti-human serum albumine/human serum albumine (α-HSA/HSA) immunoreaction demonstrates the feasibility to use the microfluidic sensing system for immunosensing applications. In this case, a better discrimination between the bulk refractive index change and the layer formation can be made, resulting into higher accuracy and offering the prospect of being able to use the kinetics of the immunoreaction. The microfluidic sensing system shows an average phase resolution of $7 \times 10^{-5} \times 2\pi$ for different pairs of channels, which at the given interaction length of 4 mm corresponds to a refractive index resolution of 6×10^{-8}, being equivalent to a protein mass coverage resolution of 20 fg/mm^2.

Keywords: Integrated optics; Multichannel Young interferometer; Microfluidics; Lab-on-a-chip; Immunosensor

1. Introduction

There is a high need for highly sensitive multichannel sensors, which are required to measure various types of analytes in different areas of applications such as e.g. health care and food industry. Interference-based integrated optical (IO) sensors such as the Mach-Zehnder interferometer (Heideman and Lambeck, 1999) and the Young interferometer (YI) (Brandenburg, 1997; Ymeti et al., 2002; Cross et al., 2003) are among the most sensitive devices reported, being able to detect refractive index changes as small as 10^{-8}. This corresponds to a protein concentration of 5.3×10^{-8} g/ml (assuming $dn/dc = 0.188$ ml/g (De Feijter et al., 1978)). The high sensitivity, combined with a fast and accurate measurement, makes these devices very attractive, e.g. for point-of-care testing and medical screening.

In order to perform a measurement with an interferometric device, it is necessary to bring the sample solutions to the sensing windows of these devices. Often for that purpose, bulky cuvette systems are used (Heideman and Lambeck, 1999; Brandenburg, 1997). These cuvettes can be made from different materials such as Teflon, Perspex, etc., and are mounted on the IO chip in various ways, e.g. by pressing or gluing them to the sensor. A drawback of these cuvette systems is the large response time, up to several minutes, due to mixing between sample solutions that are successively

* Corresponding author. Tel.: +31-53-489-3112; fax: +31-53-489-1105.
E-mail address: A.Ymeti@utwente.nl (A. Ymeti).

0956-5663/$ – see front matter © 2004 Elsevier B.V. All rights reserved.
doi:10.1016/j.bios.2004.04.015

applied to the sensing window and/or slow replacement of surface layer, both being mainly due to relatively large volume of the cuvette flow chambers (6 μl (Ymeti et al., 2002)). In addition, relatively large volumes of the samples to be monitored are needed.

Microfluidics (Ramsey and van den Berg, 2001) has been successfully implemented in various sensing platforms, e.g. in a surface plasmon resonance sensor (Schlautmann et al., 2003), evanescent wave absorption-based sensing (Pandraud et al., 2000), etc. The use of microfluidics for sensor applications has several advantages: (i) it strongly reduces the mixing time between sample solutions, resulting in a fast response of the sensor; (ii) it enables the use of small sample volumes; and (iii) it can readily be integrated with the sensor, resulting in a compact sensing system.

In this paper, we report about the integration of microfluidics and an interferometric sensor into a four-channel IO YI sensor and demonstrate its usefulness in immunosensing applications. Using microfluidics, the effect of changes in solution on the refractive index can be well separated from those due to layer formation in an immunoreaction, resulting in a better-controlled experiment and a more accurate result. In addition, exposure of the active sensor area to a contaminated environment will be avoided.

In Section 2, we describe the design and fabrication of the microfluidics and optical chips into one single integrated device. In Section 3, we will show experimental results illustrating the advantages of these sensors. Conclusions of this work will be presented in Section 4.

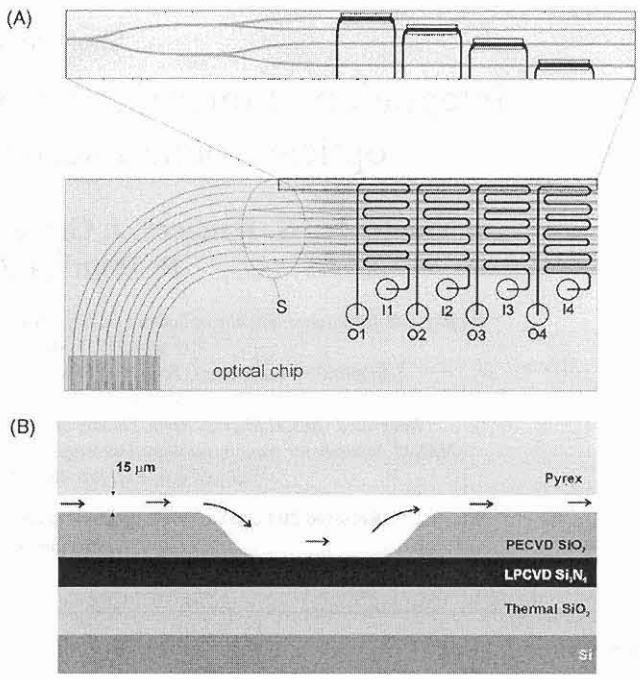

Fig. 1. Top-view (A) and cross-section along one of sensing windows (B) of the microfluidic system aligned on a four-channel IO YI chip. The optical chip contains configurations of YI sensor structure, which have different distances between their output channels, resulting in a different length of splitting function, manifested by different starting positions of the first Y-junction (see S in A). Ii and Oi indicate the input and output, respectively, of microfluidic channel *i*, addressing the *i*th bundle of sensing windows. Dimensions of the microfluidic sensing system are 63 mm × 24 mm.

2. Design and fabrication

In brief, the working principle of a four-channel YI is similar to a two-channel YI. In a two-channel YI, laser light is coupled to a guided mode of a channel waveguide and is then split into two channels: a measurement and a reference channel. At the end of the waveguide chip, the light is coupled out and the two output beams are overlapped in order to generate an interference pattern on a CCD camera. When the optical path length difference between the two channels changes, the interference pattern shifts along the CCD camera. The shift is determined by a Fast Fourier Transform (FFT) algorithm. In a four-channel YI (Fig. 1A), there are four waveguide channels positioned at different distances from each other. Since the spatial frequency of the interference pattern is related to the distance between the channels, this gives rise to different spatial frequencies and in this way provides a means to determine all six optical path length differences that occur among the four different channels. If the YI is used as an immunosensor, the determined path length differences, which are due to a change in the refractive index of the waveguide modes, are caused by protein adsorption at the waveguide surface. Proteins can access the waveguide surface only at the measuring windows where the waveguide surface is in contact with the sample solution (Fig. 1B).

The layout of the microfluidic system and the optical chip in mutual alignment is shown in Fig. 1. The optical chip contains 11 four-channel YI structures positioned parallel to each other. A detailed description of the design and fabrication of this four-channel IO YI chip is given elsewhere (Ymeti et al., 2003). Note that the interaction length of each sensor is 4 mm. The layout of the microfluidic system is adapted to the layout of the optical chip. The microfluidic system is a glass plate (Pyrex wafer with a thickness of 525 μm) in which four meander-like microchannels have been implemented. The channels are 200 μm wide, 15 μm deep, and 90 mm long. Each channel passes a bundle of 11 sensing windows, each being part of a different YI structure in the optical chip. In the glass plate, holes with diameter of 2.5 mm were drilled for connection of the channels with the outside world. The distance between two holes (center-to-center) is chosen 3.5 mm.

The channel structure was realized by means of wet etching technique using a 5% hydrochloric fluoride (HF) solution. The holes were realized by powderblasting. For attaching the microfluidic channel system to the optical YI chip, we first tested anodic bonding. For that purpose, we performed test experiments, which involve Silicon wafers

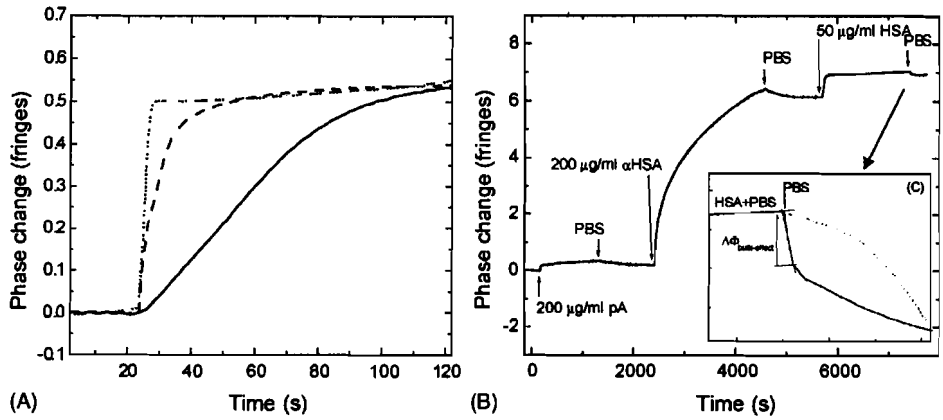

Fig. 2. (A) The response of the YI-sensing system to a π-phase-change introduced by substituting the demi-water in measuring channel 1 of the fifth YI structure from the top (see Fig. 1A) by a 0.308% (by weight) glucose solution using a bulky cuvette (solid line), a bulky cuvette with an air bubble (dashed line), and the microfluidic system (dotted line). (B) Phase change measured using the microfluidic sensing system when α-HSA/HSA interaction is taking place in the measuring channel. The inset (C) shows the time-response of the microfluidic system (solid line) when the HSA solution in the measuring channel was substituted by a PBS buffer solution at the indicated time (arrow) as well as this measurement performed with a bulky cuvette (dotted line). $\Delta\Phi_{\text{bulk-effect}}$ indicates the phase change due to the difference in bulk refractive index between HSA solution and PBS solution.

provided with the same $SiO_2/Si_3N_4/SiON$ layer stack as our samples. Due to the thick SiO_2 layer of 1.25 μm, anodic bonding was not successful. The electric resistance of SiO_2 layers with thicknesses more than 500 nm is too high for anodic bonding. However, reducing the SiO_2 layer thickness to values below 500 nm causes the evanescent field to penetrate into the highly absorbing Si, resulting in unacceptable high optical losses. Therefore, it was investigated to glue the optical chip to the microfluidic chip. A UV-curable glue was applied in such a way that no glue is present inside the fluidic channels and on the sensing windows. The glue consists of pure isobornyl acrylate to which dimethoxyfenylacetophenone (DMPA) was added (3.84% w/v). The glue selected has a low viscosity and a good biocompatibility. The low viscosity of the glue ensures formation of a thin layer after spinning. After spinning, we used a stamping method to selectively apply this glue layer to the bonding surface and to prevent contact with the channel structures. For a detailed description of the gluing procedure, we refer to Schlautmann et al. (2003).

3. Experimental results

Fig. 2A shows the response of the microfluidic sensing system to a phase change of $0.5 \times 2\pi$ introduced in measuring channel 1 of the fifth YI structure from the top (see Fig. 1A) by replacing demi-water by a 0.308% (by weight) glucose solution (Weast, 1985). The same figure also shows the response of the sensor in case our bulky cuvette is used, as well as the response using this cuvette when an air bubble is introduced as a plug in between two flowing liquids in order to prevent their mixing.

From Fig. 2A, it can be concluded that the time interval τ required to obtain a stable base line after introducing the glucose solution, is decreased by a factor of 25 (from $\tau^{\text{bulky cuvette}} = 100$ s to $\tau^{\text{microfluidics}} = 4$ s). These results can be explained by assuming there is laminar flow inside the flowcells (for both flowcells, the Reynolds number ≪2300 at the used fluid velocity of 3 cm/s). Two experimental conditions can now be distinguished: (i) the low diffusion regime, in which τ is dominated by the flow velocity in the vicinity of the sensor surface; and (ii) the fast diffusion regime, in which τ is determined by the diffusion of solvent molecules from the center of the flowchannel toward the sensor surface. First, we consider the low diffusion regime. In case of laminar flow, the fluid velocity in the region close to the waveguide surface is increased if the flowcell thickness is decreased (provided that the average velocity remains the same). An increase in velocity implies a decrease of the response time as observed in the experiment. Quantitative analysis of the average fluid velocity v_l within the layer probed by the evanescent field (which extends approximately 100 nm into the fluid) for the two different flowcells results $v_l^{\text{microfluidics}}/v_l^{\text{bulky cuvette}} = 33$. Since τ is inversely proportional to v_l, we arrive at a ratio for the time responses: $\tau^{\text{bulky cuvette}}/\tau^{\text{microfluidics}} = 33$. In the high diffusion regime, τ is by approximation proportional to the height of the flow channel. This results in $\tau^{\text{bulky cuvette}}/\tau^{\text{microfluidics}} = 500\,\mu\text{m}/15\,\mu\text{m} = 33.3$. In conclusion for both the slow and fast diffusion regime, the estimated ratio $\tau^{\text{bulky cuvette}}/\tau^{\text{microfluidics}}$ corresponds reasonably well with the value of 25 found in our experiment. Observed differences may be explained by small uncertainties in the average flow speeds between the two flowcells.

In addition, the required sample volume (1 μl) is roughly three orders of magnitude smaller compared to the volume required in case of the bulky cuvette (1 ml) for the same flow speed of 3 cm/s. For different flow speeds, the absolute volume required will be different.

The microfluidic sensing system has also been applied to monitor the α-HSA/HSA immunoreaction. Fig. 2B presents the phase changes that occur upon binding of HSA to α-HSA immobilized onto the measuring channel. The sensing protocol for this immunoreaction consists of three steps. Firstly, adsorption of protein A (pA) on the sensor surface by flowing a 200 μg/ml solution of pA in phosphate buffered saline (PBS, pH 7.35) through the channel. Application of the pA allows proper orientation of the antibody molecules for antigen binding (Owaku and Goto, 1993; Bin et al., 1996). Secondly, the antibody was bound to the pA-modified surface by flowing a 200 μg/ml solution of α-HSA prepared in PBS through the channel. Finally, a 50 μg/ml solution of HSA in PBS was applied to allow binding of HSA molecules. After each step, a washing with PBS was performed in order to remove loosely bound protein molecules and to get rid of the bulk refractive index effect. The phase changes caused by α-HSA adsorption ($6 \times 2\pi$), and binding of HSA ($0.8 \times 2\pi$) are in line with earlier results (Heideman et al., 1993). This experiment demonstrates the feasibility to use the YI sensor in combination with a microfluidic cuvette for immunosensing applications.

The reduction of response time can also be observed by analyzing the process during addition of PBS after the third step in more detail, see Fig. 2C. The curve obtained with the microfluidics shows a fast phase drop (5 s) followed by a slower decrease. The initial drop is due to the difference in refractive indices between HSA solution and PBS (referred to as the bulk effect). The slower decrease presumably arises from a gradual desorption of proteins from the sensor surface. Using bulky cuvettes, bulk effects extend over much longer times (see Fig. 2C). This normally hampers quantitative determination of reaction rates from data obtained for an immunoreaction because the value of the bulk effect cannot be easily extracted from the data if the time response of the sensor is comparable with the timescale of the bioreaction. However, with the use of microfluidics it is now possible to accurately determine the phase change of the bulk effect, making these types of sensors even more accurate.

Application of the microfluidic system appears not to influence the phase resolution, being $7 \times 10^{-5} \times 2\pi$ and $1 \times 10^{-4} \times 2\pi$ for the sensing system with and without the microfluidic system, respectively. Taking into account the value of interaction length (4 mm), this corresponds to a refractive index resolution of 6×10^{-8}, which is equivalent to a protein mass coverage resolution of 20 fg/mm^2.

4. Conclusions

A microfluidic system was designed, fabricated, and mounted to a four-channel IO YI sensor chip. The microfluidic system consists of a Pyrex wafer in which four microchannels with cross-sectional dimensions of 200 μm × 15 μm have been implemented, each of them addressing a set of 11 sensing windows one in each of the four-channel YI structures realized on top of a Silicon chip. The microfluidic system was bonded to the optical YI chip by means of a gluing technique.

It is shown that the response time needed to achieve a stable signal at replacing demi-water by a glucose solution corresponding to a π-phase change is 4 s, implying a drastically reduced value when compared to that achieved by using a bulky cuvette (100 s). This result can be explained qualitatively and quantitatively by assuming laminar flow inside the flowcells. In addition, the volume of the sample solution required to perform an immuno-test is two to three orders of magnitude smaller than that using a bulky cuvette-based system. The monitoring of the α-HSA/HSA immunoreraction shows that by using a microfluidic system, a better discrimination between bulk effects, due to refractive index difference of both solutions, and the layer formation can be made. This expectedly results into higher accuracy and offers the prospect of investigating or using the kinetics of the immunoreaction.

The microfluidic sensing system shows a phase resolution of $7 \times 10^{-5} \times 2\pi$, which corresponds to a refractive index resolution of 6×10^{-8}, being equivalent to a protein mass coverage resolution of 20 fg/mm^2. The combination of the microfluidics with the highly sensitive multichannel YI device is a very attractive system, which can be effectively used in medical screening, food analysis, etc., as a new lab-on-a-chip configuration.

Acknowledgements

This project was financially supported by the Dutch Technology Foundation (Technologiestichting) STW. We gratefully acknowledge helpful discussions with Dr. R.B.M. Schasfoort. The protein A, anti-human serum albumine (α-HSA), and human serum albumine (HSA) were a kind gift from T. Wink, Paradocs bv, Tiel, The Netherlands.

References

Bin, L., Smyth, M.R., O'Kennedy, R., 1996. Oriented immobilization of antibodies and its applications in immunoassays and immunosensors. Analyst 121, 29R–32R.

Brandenburg, A., 1997. Differential refractometry by an integrated-optical Young interferometer. Sens. Actuators B 38-39, 266–271.

Cross, G.H., Reeves, A.A., Brand, S., Popplewell, J.F., Peel, L.L., Swann, M.J., Freeman, N.J., 2003. A new quantitative optical sensor for protein characterization. Biosens. Bioelectron. 19, 383–390.

De Feijter, J.A., Benjamins, J., de Veer, F.A., 1978. Ellipsometry as a tool to study the adsorption behavior of synthetic and biopolymers at the air-water interface. Biopolymers 17, 1759–1772.

Heideman, R.G., Kooyman, R.P.H., Greve, J., 1993. Performance of a highly sensitive optical waveguide Mach-Zehnder interferometer immunosensor. Sens. Actuators B 10, 209–217.

Heideman, R.G., Lambeck, P.V., 1999. Remote opto-chemical sensing with extreme sensitivity: design, fabrication and performance of a pigtailed integrated optical phase-modulated Mach-Zehnder interferometer system. Sens. Actuators B 61, 100–127.

Owaku, K., Goto, M., 1993. Optical Immunosensing for IgG. Sens. Actuators B 13-14, 723–724.

Pandraud, G., Koster, T.M., Gui, C., Dijkstra, M., van der Berg, A., Lambeck, P.V., 2000. Evanescent wave sensing: new features for detection in small volumes. Sens. Actuators A 85, 158–162.

Ramsey, J.M., van den Berg, A., 2001. Micro Total Analysis Systems, Kluwer, Dordrecht.

Schlautmann, S., Besselink, G.A.J., Prabhu, R., Schasfoort, R.B.M., 2003. Fabrication of a microfluidic chip by UV bonding at room temperature for integration of temperature sensitive layers. J. Micromech. Microeng. 13, 81–84.

Weast, R.C., 1985. Handbook of Chemistry and Physics, 65th ed. CRC Press, Boca Raton, p. D-234.

Ymeti, A., Kanger, J.S., Wijn, R., Lambeck, P.V., Greve, J., 2002. Development of a multichannel integrated interferometer immunosensor. Sens. Actuators B 83, 1–7.

Ymeti, A., Kanger, J.S., Greve, J., Lambeck, P.V., Wijn, R., Heideman, R.G., 2003. Realization of a multichannel integrated Young interferometer chemical sensor. Appl. Opt. 42, 5649–5660.